Protein Science (1992), *1*, 1585–1594. Cambridge University Press. Printed in the USA.

Crystal structure of the Y52F/Y73F double mutant of phospholipase A_2: Increased hydrophobic interactions of the phenyl groups compensate for the disrupted hydrogen bonds of the tyrosines

CHANDRA SEKHARUDU,[1,3] BOOPATHY RAMAKRISHNAN,[1,3] BAOHUA HUANG,[1] RU-TAI JIANG,[1] CYNTHIA M. DUPUREUR,[1,4] MING-DAW TSAI,[1,2] AND MUTTAIYA SUNDARALINGAM[1,2,3]

[1] Laboratory of Biological Macromolecular Structure, Department of Chemistry, [2] Department of Biochemistry, and [3] Ohio State Biotechnology Center, The Ohio State University, Columbus, Ohio 43210

(RECEIVED June 17, 1992; REVISED MANUSCRIPT RECEIVED August 10, 1992)

Abstract

The enzyme phospholipase A_2 (PLA2) catalyzes the hydrolysis of the sn-2 ester bond of membrane phospholipids. The highly conserved Tyr residues 52 and 73 in the enzyme form hydrogen bonds to the carboxylate group of the catalytic Asp-99. These hydrogen bonds were initially regarded as essential for the interfacial recognition and the stability of the overall catalytic network. The elimination of the hydrogen bonds involving the phenolic hydroxyl groups of the Tyr-52 and -73 by changing them to Phe lowered the stability but did not significantly affect the catalytic activity of the enzyme. The X-ray crystal structure of the double mutant Y52F/Y73F has been determined at 1.93 Å resolution to study the effect of the mutation on the structure. The crystals are trigonal, space group $P3_121$, with cell parameters $a = b = 46.3$ Å and $c = 102.95$ Å. Intensity data were collected on a Siemens area detector, 8,024 reflections were unique with an R(sym) of 4.5% out of a total of 27,203. The structure was refined using all the unique reflections by XPLOR to a final R-factor of 18.6% for 955 protein atoms, 91 water molecules, and 1 calcium ion. The root mean square deviation for the α-carbon atoms between the double mutant and wild type was 0.56 Å. The crystal structure revealed that four hydrogen bonds were lost in the catalytic network; three involving the tyrosines and one involving Pro-68. However, the hydrogen bonds of the catalytic triad, His-48, Asp-99, and the catalytic water, are retained. There is no additional solvent molecule at the active site to replace the missing hydroxyl groups; instead, the replacement of the phenolic OH groups by H atoms draws the Phe residues closer to the neighboring residues compared to wild type; Phe-52 moves toward His-48 and Asp-99 of the catalytic diad, and Phe-73 moves toward Met-8, both by about 0.5 Å. The closing of the voids left by the OH groups increases the hydrophobic interactions compensating for the lost hydrogen bonds. The conservation of the triad hydrogen bonds and the stabilization of the active site by the increased hydrophobic interactions could explain why the double mutant has activity similar to wild type. The results indicate that the aspartyl carboxylate group of the catalytic triad can function alone without additional support from the hydrogen bonds of the two Tyr residues.

Keywords: hydrophobic interactions compensate hydrogen bonds; phospholipase A_2 Y52F/Y73F double mutant; similar enzymatic activity of double mutant and wild type; structure–activity relationship; X-ray crystal structure

Reprint requests to: Muttaiya Sundaralingam, Room 12, Rightmire Hall, Biotechnology Center, The Ohio State University, Columbus, Ohio 43210.

[4] Present address: Department of Chemistry, California Institute of Technology, Pasadena, California 91125.

As a part of our continuing studies on the structure–activity relationships of the enzyme phospholipase A_2(PLA2) from bovine pancreas (Noel et al., 1991), we report the structure of the double mutant (Y52F/Y73F) where the

Tyr residues 52 and 73 are mutated to Phe (Kinemage 1). In the wild-type (WT) PLA2, the catalytic triad consists of the residues Asp-99, His-48, and a water molecule, which are hydrogen bonded to each other (Fig. 1; Kinemage 1). The carboxylate group of Asp-99 is also hydrogen bonded to a second water molecule in the interior of the catalytic "pocket," which is in turn hydrogen bonded to the carbonyl oxygen of Pro-68, NH_3^+ of Ala-1, and OH of Tyr-52. The Asp-99 carboxylate group is also involved in two additional hydrogen bonds with the hydroxyl groups of the two invariant tyrosine residues, 52 and 73 (Verheij et al., 1981; Maraganore et al., 1987; van den Bergh et al., 1987) (Fig. 1). Furthermore, Tyr-73 directly interacts with the N-terminal helix that is involved in the interfacial catalysis (Dijkstra et al., 1981a). The complex network of hydrogen bonds (Brunie et al., 1985) was believed to stabilize the catalytic pocket and was thought to be the reason for the high conservation of the two Tyr residues 52 and 73 in both the class I and II families of PLA2s (Heinrikson et al., 1977) except bee venom PLA2, which has only one analogous Tyr (Scott et al., 1990). Despite all of these indications of the potential importance of Tyr-52 and Tyr-73 on the structure and function of PLA2, the kinetic behavior of the Y52F/Y73F mutant is similar to that of WT PLA2 (Dupureur et al., 1992b). A possible explanation for the high activity of the double mutant is that perhaps additional solvent water molecules replace the phenolic hydroxyl groups in the active site. To gain insights into the structural effects of the mutations on the catalytic site and the N-terminal helix, we have determined the crystal structure of the trigonal form of the double mutant and compared it with the trigonal form of the WT determined earlier (Noel et al., 1991). The structure of the Y52F/Y73F double mutant reveals that in the absence of the hydrogen bonds involving the phenolic hydroxyl groups the catalytic site is stabilized by hydrophobic interactions.

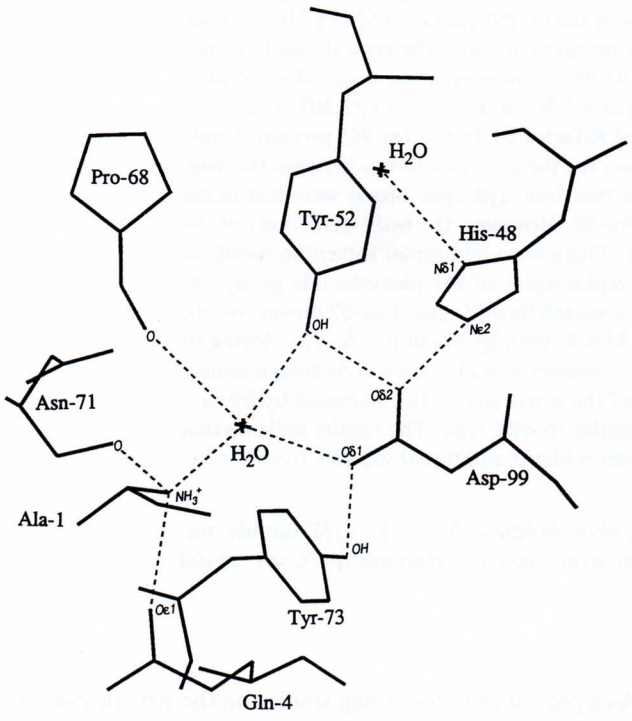

Fig. 1. Hydrogen-bonding interactions involving the Tyr-52, Tyr-73, structural water molecule, and the catalytic triad based on the wild type structure.

Results and discussion

The root mean square (rms) deviations in the bond distances (0.012 Å) and other stereochemical parameters (Table 1) suggest that the model has good stereochemistry. The Ramachandran plot showing the distribution of the (ϕ, ψ) angles is given in Figure 2. All the non-glycine residues are within the allowed region. In the final structure, all atoms have unit occupancy and individual isotropic B (Å^2) values. The average B values for the various parts of the model are listed in Table 1. The two regions that exhibit high $\langle B \rangle$ values greater than 50 Å^2, 62–66 and 116–121, have weak electron density. Both these segments are accessible to solvent in the crystal. Further, both these regions are remote to the functional regions such as the calcium-binding site or the catalytic site. The electron densities computed with phases of the final model consisting of the mutated residues are shown in Figure 3. The double mutant structure is compared in detail with our WT structure (Noel et al., 1991).

Overall structure

The rms difference for all the α-carbon atoms between WT and Y52F/Y73F structures is 0.56 Å. The two struc-

Table 1. *Crystal data and the root mean square (rms) deviations in the geometric parameters*

Space group	$P3_121$
Cell	$a = b = 46.30$ Å and $c = 102.95$ Å
Resolution limits	6.0–1.93 Å
Reflections	8,024 ($F > 1.0\sigma$)
Crystallographic R-factor	0.186
Number of protein atoms	955
Number of bound ions	1 Ca^{2+}
Number of solvent molecules	91
Geometric conformity (rms in the structure)	
Bond lengths	0.012 Å
Bond angles	2.837°
Chiral volumes	0.140 Å^3
Deviations from planarity (ω)	8.750°
Deviations from the planarity	1.834°
Average positional error	≈0.2 Å
Temperature factors of the refined structure	
Main chain	17.9 Å^2
Side chains	21.1 Å^2
Solvent	38.0 Å^2
Calcium ion	13.1 Å^2

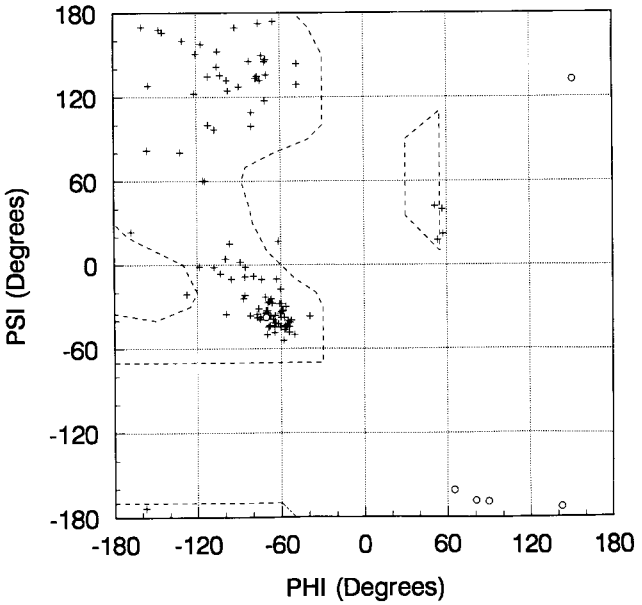

Fig. 2. Ramachandran map for the double mutant Y52F/Y73F, of phospholipase A_2. The backbone phi, psi angles for non-glycines are denoted by + and for glycines by O.

tures are similar as seen from the superposition of the α-carbon trace of the WT on the mutant structure (Fig. 4); there are no backbone segments that radically differ in their conformation. The high degree of conservation in the overall structure is remarkable because of the dramatically increased conformational flexibility indicated by NMR (Dupureur et al., 1992a; Y. Li et al., unpubl.) and 50% loss in conformational stability compared to the WT (Dupureur et al., 1992b) contrary to expectations. There is no evidence of additional solvent molecules at the active site in place of the hydroxyl groups. The crucial hydrogen bonds involving the catalytic triad are conserved, which may explain the WT activity of the double mutant. However, significant conformational and positional changes are observed in the side chains near the sites of mutation compared to WT. These conformational changes are found to be related to the removal of the phenolic hydroxyl groups.

At the mutation sites

Tyr-73 → Phe-73

In WT PLA2, Tyr-73 forms a direct hydrogen bond to the carboxylate group of the catalytic residue Asp-99 and is interdigitated between residues Met-8 and Gln-4 of the N-terminal helix and Ile-95, Cys-96, and Asp-99 of the E-helix. These crucial van der Waals interactions between the two helices and Tyr-73 appear to be important for the stability of the structure and catalytic activity of PLA2. Besides these residues, Tyr-75 also interacts with Tyr-73 in a face-to-edge fashion (Fig. 5a; Kinemage 2). The four residues, viz., Ile-95, Met-8, Tyr-75, and Asp-99, are in contact with the edges of Tyr-73 in the plane of the phenyl ring (Fig. 5a), whereas the other two residues, Cys-96 and Gln-4, are on either side of the Tyr ring sandwiching it (Fig. 5b). The in-plane van der Waals interactions, the hydrogen bonding between the η-hydroxyl group of 73, and the carboxylate oxygen of 99 severely restrict the χ^1 rotation angle of 73. The residue Cys-96 that is rigidly held by the S-S bridge and by Gln-4 restricts the rotation around the χ^2 angle of Tyr-73. Thus in WT, the bulk of the aromatic residue Tyr-73 stabilizes the catalytic site and the two helices: the N-terminal A-helix, which is implicated in interfacial recognition, and the E-helix that carries the catalytic residue Asp-99.

In the double mutant Y52F/Y73F, some small but significant and correlated changes are observed around Phe-73. As in WT, the residues Ile-95, Met-8, Tyr-75, Cys-96, Asp-99, and Gln-4 are in contact with Phe-73 (Fig. 5c,d; Kinemage 2). However, the absence of the hydrogen bond between the hydroxyl group of 73 and the carboxylate oxygen of 99 brings these two residues closer together by about 0.4 Å and bridges the gap between them (Table 2). This results in the negatively charged carboxylate group making van der Waals interactions with the aromatic phenyl ring (Fig. 5c). Also, the absence of the η-hydroxyl group in 73 draws Met-8 closer (by 0.5 Å) to the aromatic ring compared to WT (Table 2). The residues 95 and 75 on either side of the phenyl ring of 73 are not disturbed (Fig. 5d). As expected, the χ^1 and χ^2 dihedral angles of these residues are similar to WT. Thus, although the mutation Tyr-73 → Phe-73 has produced some local conformational perturbations, the interactions between 73 and its neighborhood are essentially conserved, particularly the interdigitation between the N-terminal and E-helices.

Tyr-52 → Phe-52

In WT, the η-hydroxyl group of Tyr-52 forms two hydrogen bonds, one with the carboxylate group of the catalytic Asp-99 and the other with the active site water molecule. The aromatic ring of 52 is anchored in its plane by Cys-98 and Pro-68 (Fig. 6a; Kinemage 3) and sandwiched by His-48 and Ile-95 (Fig. 6b). Removal of the hydroxyl group by mutating Tyr-52 → Phe-52, again, did

Table 2. *Comparison of contact distances in the wild type and the double mutant involving the mutated residues*

Atom (residue)	Atom (residue)	Distance in wild type (Å)	Distance in double mutant (Å)
Cζ (73)	Oδ1 (99)	3.4	3.0
Cζ (73)	Cε (8)	4.0	3.5
Cζ (52)	Nε2 (48)	3.9	3.3
Cζ (52)	Oδ2 (99)	3.5	3.0

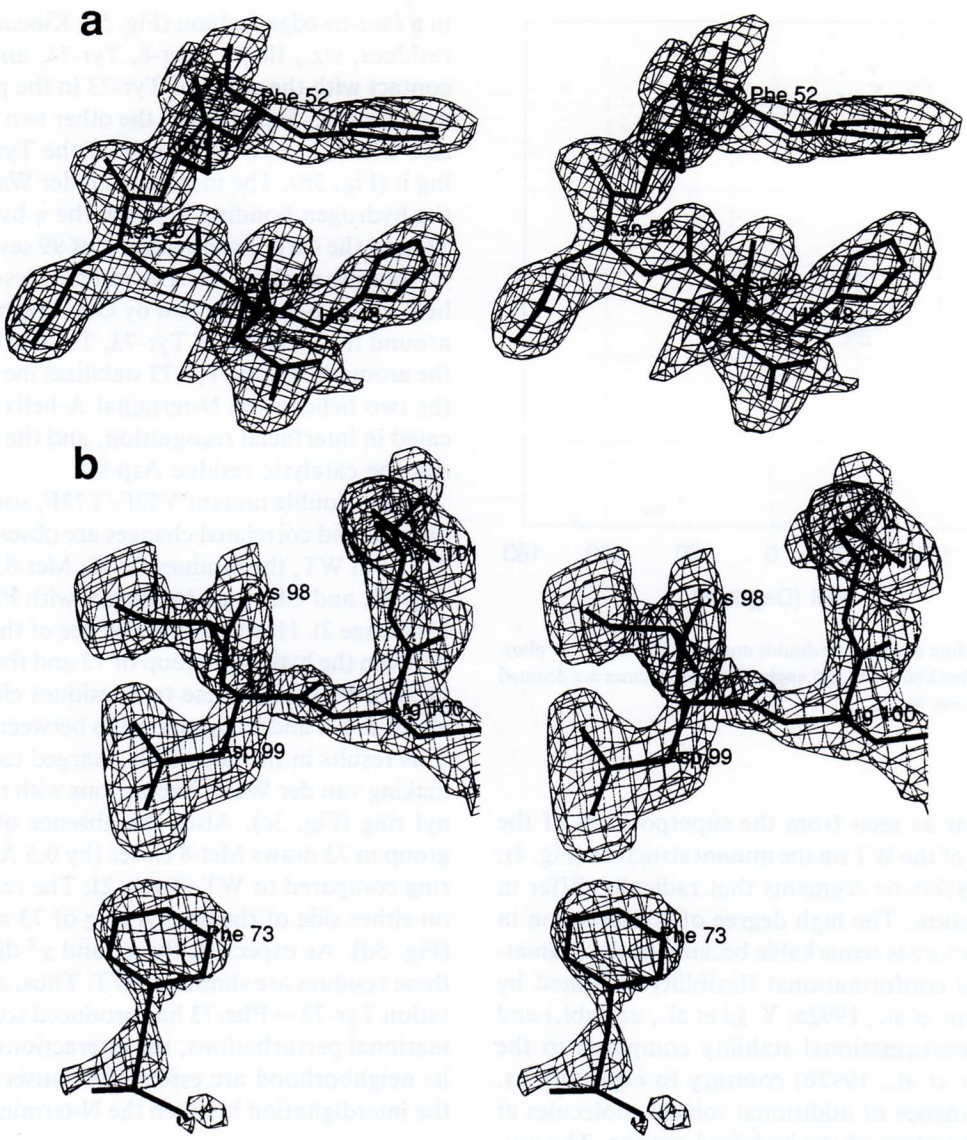

Fig. 3. **a**: Electron density over the segment 48–52 in the Sim-weighted $2F_o - F_c$ omit maps contoured at 1.5σ level. **b**: The $2F_o - F_c$ omit maps for the residue Phe-73 and the segment 98–101.

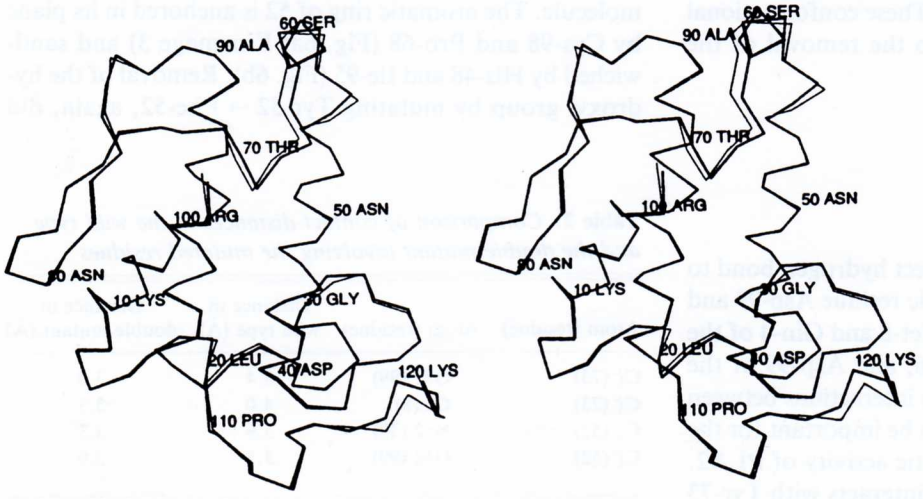

Fig. 4. Alpha-carbon trace of the wild-type phospholipase A_2 (thin lines) superimposed on the alpha-carbon trace (thick lines) of the double mutant Y52F/Y73F.

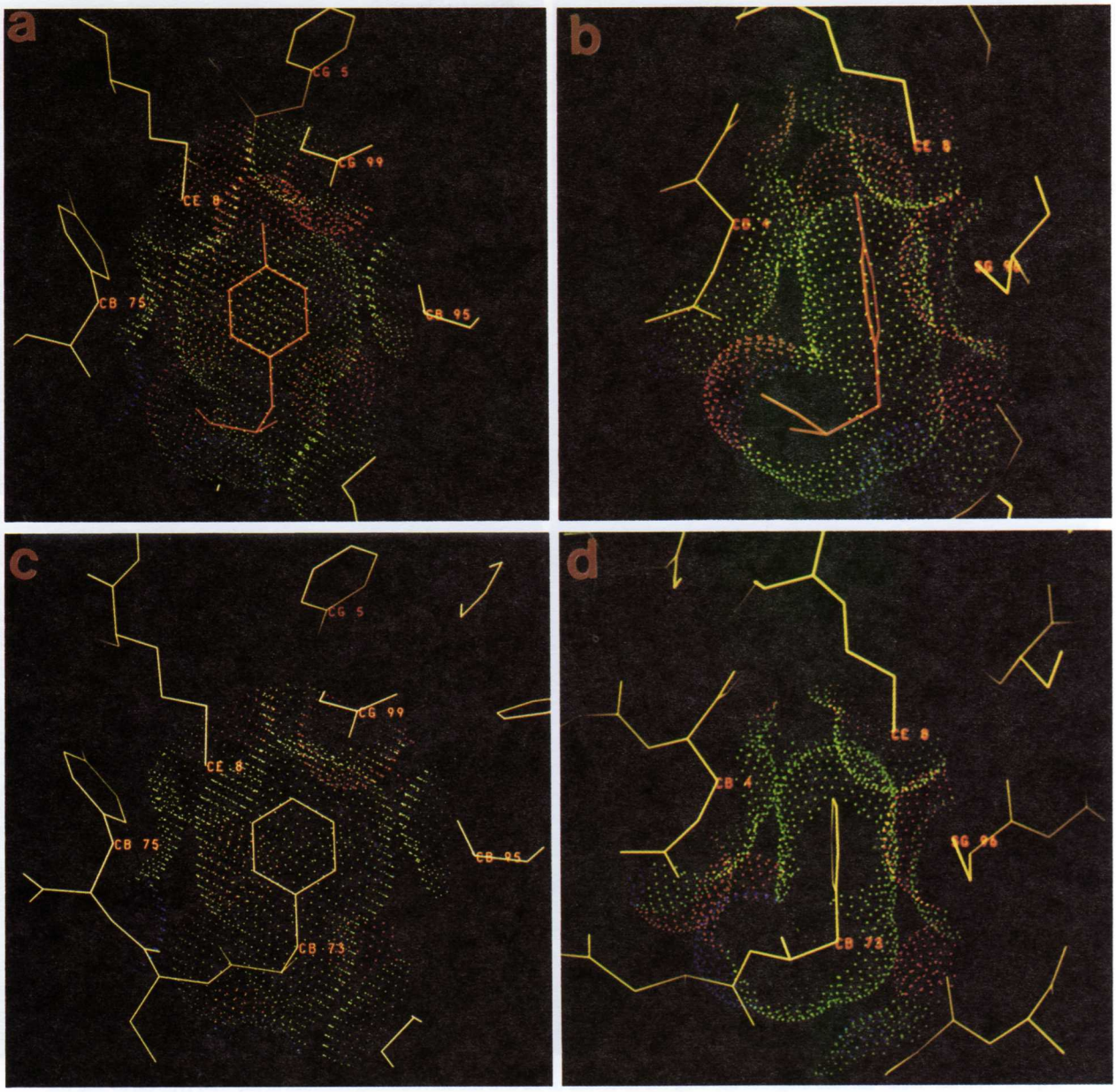

Fig. 5. Van der Waals surface diagram showing the interface of 73 and the surrounding residues in the wild type (**a**, **b**) and the double mutant Y52F/Y73F (**c**, **d**) of phospholipase A_2. The close approach of the negatively charged carboxylate group of 99 to the Phe-73 in the plane (c) of the ring can be understood from the consideration of the partial electronic charge distribution in the phenyl ring. Although the faces of the aromatic ring are covered with the δ^- π electron cloud, the δ^+ charge of the hydrogen atoms bound to each of the ring carbon atoms make the edge of the planar structure positively charged. Therefore, it is favorable for the negatively charged carboxylate group to move into van der Waals interactions to the edge of the phenyl ring plane. The Cys and Met residues are known to be very vulnerable to chemical attack by free radicals. The sulfur–aromatic interactions between Met-8, Cys-96, and Phe-73 not only stabilize the structure but also reduce the solvent accessibility of the sulfur atoms. The sulfur atom of Met-8 interacts edge-on with the aromatic ring in a manner similar to the oxygen atoms, whereas Cys-96 interacts face-on.

not produce a gap between the residue 52 and the catalytic residue 99 (Fig. 6c). The structural water molecule that bridges OH (Tyr-52), Oδ1 (Asp-99), NH_3^+ (Ala-1), and the carbonyl O (Pro-68) in WT moves away from Phe-52 because it cannot form a hydrogen bond to it. This brings Phe-52 into van der Waals interaction range with Asp-99 (Table 2) and His-48 of the catalytic diad. This results in a noticeable change in the inclination of the phenyl ring toward His-48, thus increasing the van der Waals interactions (Table 2). All of these small movements enhance the van der Waals interactions among the residues of the catalytic pocket of the mutant (Fig. 6d). The in-

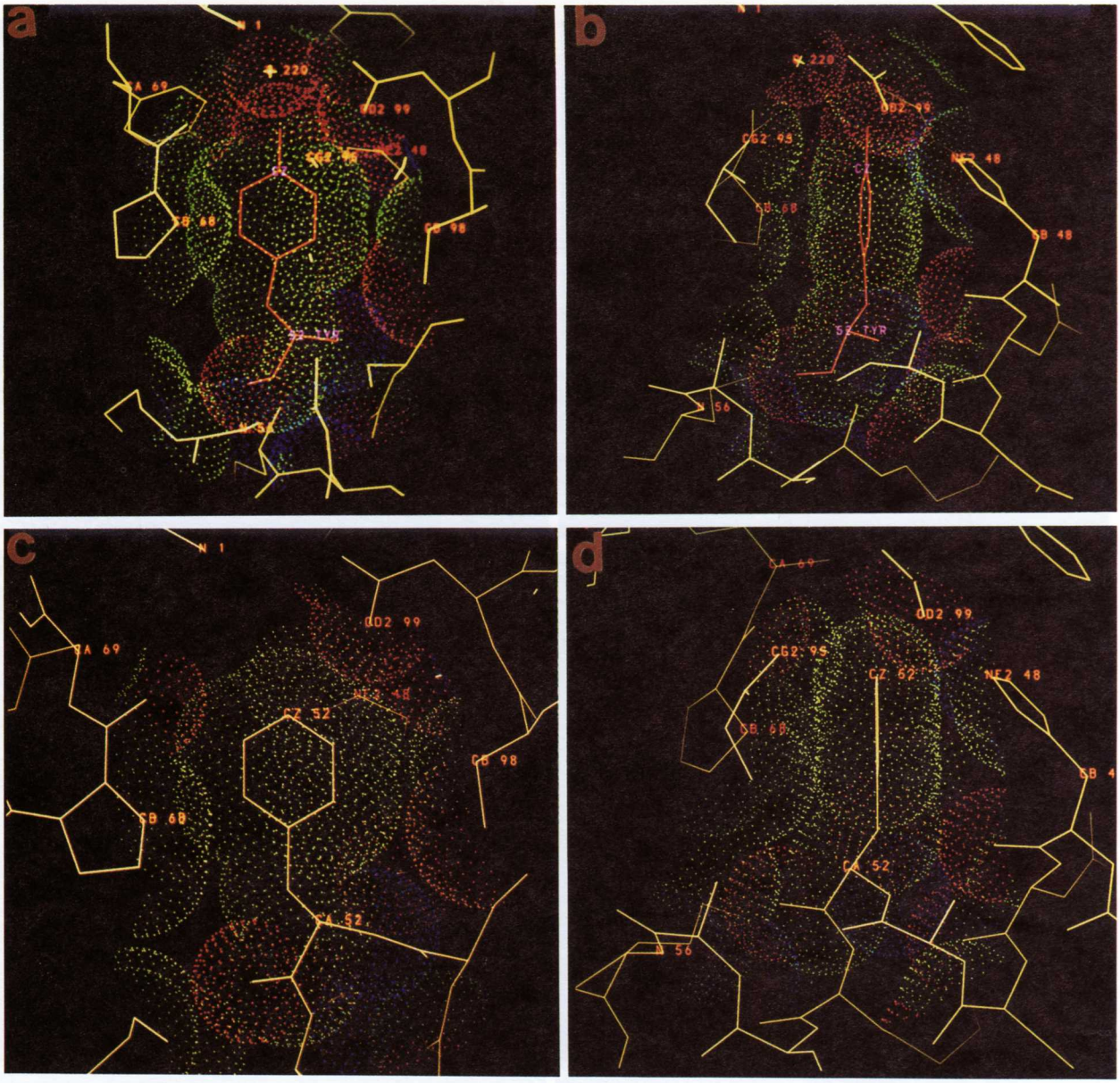

Fig. 6. Van der Waals surface diagram showing the interface of 52 and the surrounding residues in the wild type (**a**, **b**) and the double mutant Y52F/Y73F (**c**, **d**) of phospholipase A_2.

creased hydrophobic interactions probably compensate for the loss of the hydrogen bond involving the OH group of 52. The van der Waals interactions between Tyr-52, Ile-95, and Pro-68 are similar to WT. In order to conserve the van der Waals interactions in the mutant, these residues exhibit correlated movements. The only residue that is in contact with 52 and exhibits no tendency to move is Cys-98, which is involved in a disulfide bond. Ile-95 is unique in that it interacts with both the mutated residues 52 and 73 and lies at the tips of the two Tyr rings in the WT structure. The absence of the two phenolic hydroxyl groups in the mutant structure allows a larger overlap of the two aromatic groups and Ile-95.

Catalytic site

To gain insights into the effect of the above conformational perturbations on the enzymatic activity, we have closely examined the catalytic site, the N-terminus, and the putative interfacial binding loci on the surface of the enzyme. The catalytic pockets of the mature and proenzymes from a variety of species are known to be remarkably similar in the crystals. Although Phe-52 and Phe-73 in Y52F/Y73F move closer to the catalytic diad (Asp-99, His-48) compared to WT, the network of hydrogen bonds involving His-48, Asp-99, and the water molecule are conserved (Fig. 7). In both WT and the mu-

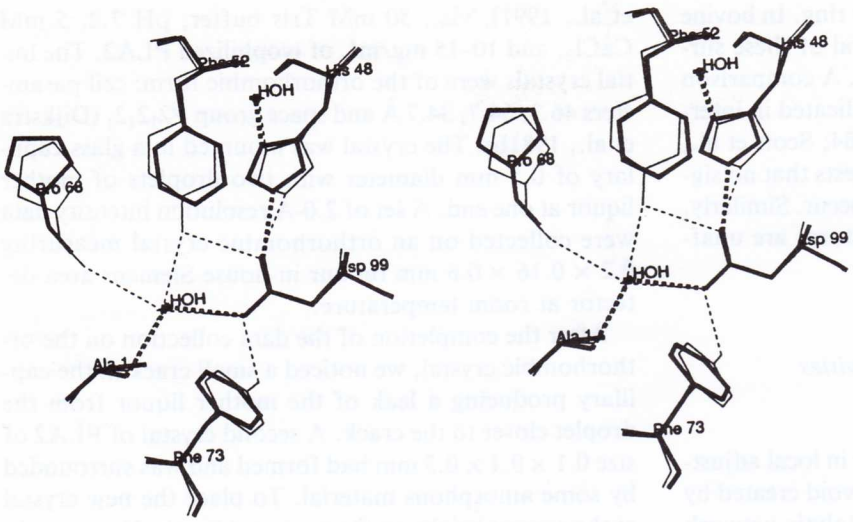

Fig. 7. Superposition of the catalytic network of Y52F/Y73F (thick bonds) on the wild type (thin bonds). The root mean square (rms) deviation for the catalytic triad is 0.235 Å. When the common atoms of the mutated residues are included, the rms is 0.33 Å.

tant, His-48 forms two hydrogen bonds, one with Asp-99 and the other with the water molecule. In turn, Asp-99 forms four hydrogen bonds in the WT, whereas it forms only two in the mutant. As mentioned above, the increased van der Waals interactions involving the phenyl groups in the mutant keep Asp-99 in the same place as in WT. The Y52F/Y73F structure has shown that despite the disruption of the four hydrogen bonds, the increased hydrophobic interactions support the hydrogen-bonding network involving the catalytic residues. This would explain the lack of perturbation in the catalytic activity.

The effect of mutation on the interfacial binding

For the enzymatic activity, which involves the combined interfacial binding and the catalytic step, the A-helix and the N-terminus apparently have to be held rigidly in place in the enzyme (Dijkstra et al., 1984). Minor modification of the N-terminus such as transamination or switching the chirality at C_α atom of Ala-1 to the D configuration dramatically decreases the potency of PLA2 binding to the lipid–water interface and therefore the lipolysis activity of PLA2 as well (Dijkstra et al., 1984). Residue 73 is in direct contact with the buried portion of the first two turns of the A-helix. However, the mutation of Tyr to Phe at 73 did not alter interactions with the A-helix. This is because only the aromatic moiety of residue 73 in both WT and Y52F/Y73F is in contact with the interior residues (Gln-4 and Met-8) of the A-helix and the E-helix surface containing residues Ile-95, Cys-96, and Asp-99 (Fig. 8; Kinemages 1, 2). This cementing role of 73 appears to be crucial in bringing the A- and E-helices into juxtaposition and at the same time stabilizing the A-helix and enabling the residues Leu-2, Trp-3, and Asn-6 to be accessible to the interfacial surface. The mutation also does not affect the interactions of the N-terminus. In the double mutant, the NH_3^+ group of Ala-1 of the N-terminus is totally inaccessible to solvent and forms three intramolecular hydrogen bonds: one to the carbonyl oxygen of Asn-71, the second to the structural water that bridges Asp-99 in the catalytic site, and the third to the $O_{\epsilon 1}$ atom of Gln-4. These interactions are similar to those observed in WT. In contrast, Tyr-52 is remote to the A-helix and the N-terminus and is not expected to influence interfacial interactions. In the crystal structures of venom PLA2–inhibitor complexes, the fatty acid chains of the inhibitor molecule are bound to the apolar channel of the enzyme. The surface residues lining the rim of the channel, besides the N-terminus and the A-helix, are also implicated in interfacial catalysis (Dijkstra et al., 1981b, 1984; Scott et al., 1990). Both mutated residues are in

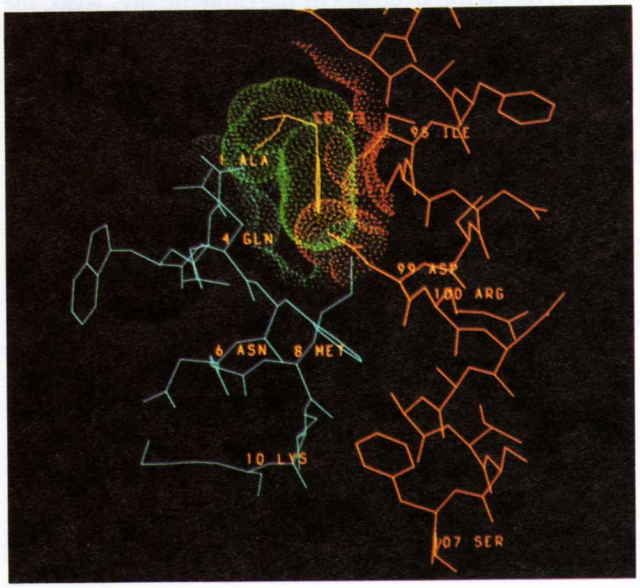

Fig. 8. Interdigitation of Phe-73 between the A-helix and the E-helix in phospholipase A_2.

van der Waals interactions with this outer ring. In bovine PLA2, unlike the venom enzymes, several of these surface residues of the outer ring are mobile. A comparison of the conformations of the residues implicated in interfacial binding (Dijkstra et al., 1981b, 1984; Scott et al., 1990) in the double mutant and WT suggests that no significant changes in the interfacial surface occur. Similarly, the calcium-binding site in the two structures are unaffected.

Possible rationalization for the low activities of nonaromatic mutants

Substitution of Tyr-73 by Phe results only in local adjustments where the residues move to fill the void created by the hydroxyl groups and conserve the catalytic network and the interfacial binding loci. However, substitution of Tyr-73 by Ala or Ser reduces the catalytic activity ($k_{cat,app}$) by two to three orders of magnitude (Dupureur et al., 1992b). This can be rationalized because the void created by the entire phenyl group (Fig. 9) cannot be filled by these smaller aliphatic residues. In contrast, Lys at position 73 can fill, to a large extent, the void left by the phenyl groups; however, the repulsion between the positively charged ϵ-ammonium group of K73 and the N-terminal ammonium group of Ala-1 probably destabilizes the enzyme, leading to the drastic decrease in enzymatic activity. Therefore the Ala and Ser mutants on one hand, and Lys on the other, reduce the enzymatic activity, but probably by different mechanisms.

In conclusion, our structural studies suggest that although the stability of the Y52/Y73 mutant is decreased due to the loss of hydrogen bonds, the hydrophobic interactions provide enough support to the protein framework to retain the structure of the catalytic site. Also, the aromatic groups, whether it be Phe or Tyr, are important for maintaining the structure and stability of the catalytic site, but also the interfacial binding site. Therefore the double mutant displays similar enzymatic activity as the wild type.

Materials and methods

Crystallization and intensity data collection

The recombinant bovine pancreatic PLA2 double mutant, Y52F/Y73F, was prepared, purified, and assayed against a variety of monomer, micellar, and vesicle substrates (Dupureur et al., 1992b). The crystals were grown at room temperature employing batch and vapor-phase methods and the conditions outlined in our previous paper (Noel et al., 1991), viz., 50 mM Tris buffer, pH 7.2, 5 mM $CaCl_2$, and 10–15 mg/mL of lyophilized PLA2. The initial crystals were of the orthorhombic form: cell parameters 46.3, 64.7, 34.7 Å and space group $P2_12_12_1$ (Dijkstra et al., 1981b). The crystal was mounted in a glass capillary of 0.5 mm diameter with two droplets of mother liquor at one end. A set of 2.0-Å resolution intensity data were collected on an orthorhombic crystal measuring $0.2 \times 0.16 \times 0.6$ mm on our in-house Siemens area detector at room temperature.

After the completion of the data collection on the orthorhombic crystal, we noticed a small crack in the capillary producing a leak of the mother liquor from the droplet closer to the crack. A second crystal of PLA2 of size $0.1 \times 0.1 \times 0.3$ mm had formed and was surrounded by some amorphous material. To place the new crystal at the correct height on the goniastat for the X-ray work, the crystal was moved away from the amorphous surroundings, and the capillary was resealed and remounted at the other end. X-ray diffraction work showed that this crystal belonged to the trigonal system, space group $P3_121$, with unit cell parameters $a = b = 46.3$ Å and $c = 102.95$ Å, which is isomorphous to our WT PLA2 (Noel et al., 1991). A complete set of intensity data on this crystal was collected out to a resolution of 1.93 Å on our Siemens area detector mounted on the four-circle goniometer. The rotating anode source was operated at 50 kV and 90 mA. The crystal-to-detector distance was 12 cm, the collimator size was 0.3 mm, and the exposure time was 90 s per frame. The data collection involved a total of three scans: one Φ scan and two ω scans. In the Φ scan, the angle was varied from 0 to 180° with an increment of 0.2°. In the $\omega 1$ scan, with $\chi = 45°$ and $\Phi = 0°$, ω was varied from 11 to 302° with an increment of −0.2°. The settings in the $\omega 2$ scan were $\chi = 45°$ and $\Phi = 60°$. From the three scans, 27,203 reflections were collected, of which 8,024 reflections ($F \geq 1\sigma$) were unique with an overall R(sym) of 4.49%. The XENGEN 1.3 software package (Howard, 1988) was used to reduce the intensity data.

Structure analysis and refinement

The unit cell parameters ($a = b = 46.3$ Å, $c = 102.95$ Å) of the double mutant were similar to the wild type ($a = b = 46.52$ Å, $c = 102.2$ Å), except the c was 0.75 Å longer. The initial model for the double mutant was obtained by mutating the Tyr residues 52 and 73 of the WT structure (Noel et al., 1991) to Phe residues. The structure determination was straightforward since the mutant crystal was isomorphous to that of WT. The starting structure was obtained by placing the mutated WT coordinates in the mutant PLA2 trigonal cell. This gave an R factor of

Fig. 9. Van der Waals surface diagrams showing the void created by mutating Tyr-73 to either (**a**) Ala, (**b**) Ser, or (**c**) Lys by modeling. The view is similar to that in Figure 5.

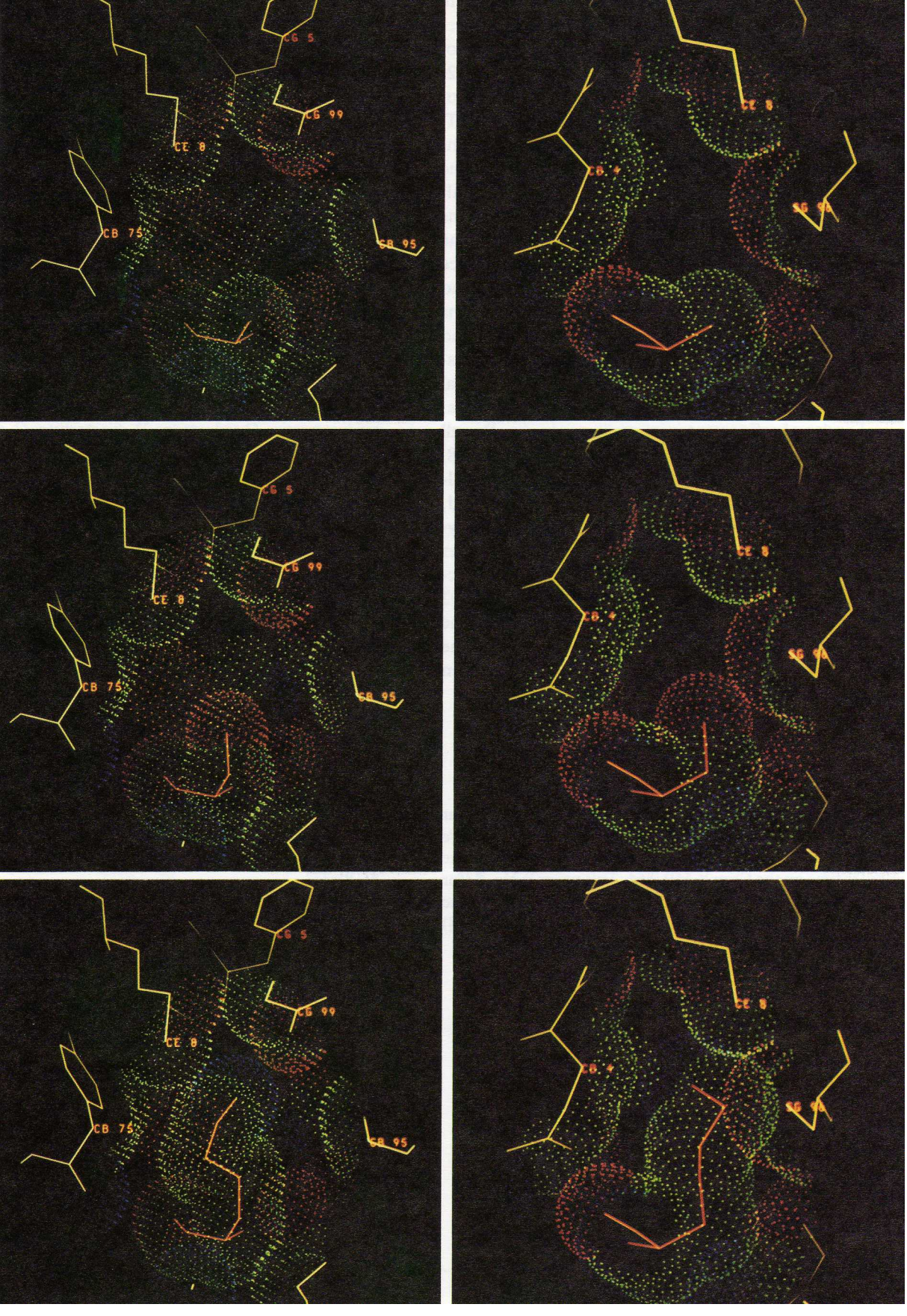
CG 5
CG 99
CE 8
CB 75
CB 95
CE 8
CB 4
SG 99

0.38 for 2,140 reflections between 6.0 and 3.0 Å resolution. After a rigid body refinement, using X-PLOR 2.1 (Brunger, 1990), the R value dropped to 0.268. The geometric center of the molecule was shifted by 0.03, 0.12, 0.62 Å in the x, y, z directions, respectively, and the molecular orientation was rotated by 1° compared to WT. When the data were extended to 2.0 Å resolution to include 7,024 reflections between 6.0 and 2.0 Å, the R value increased to 0.278. On refinement by simulated annealing, the R factor dropped to 0.212, with 6,900 reflections between 5.0 and 2.0 Å. Next, a systematic refitting of the model was carried out, using Sim-weighted difference electron-density omit maps computed with $2F_o - F_c$ and $F_o - F_c$ as coefficients and FRODO 6.6 on the Evans and Sutherland molecular graphics systems PS330 and ESV30. The maps were calculated omitting about 10 residues at a time from the N-terminal end to the C-terminal end. After the entire molecule was refitted to the maps, several cycles of refinement were performed using Powell minimization in X-PLOR 2.1, giving an R value of 0.208. At this point, difference electron-density maps were calculated to locate the water molecules. In the initial round, 49 water molecules were located. After repeating the cycle of refinement and map fitting, 92 solvent molecules were located. In the final cycles of refinement, the structure contained 955 protein atoms, 1 calcium ion, and 92 water molecules, and the R-factor was 18.6% for the 8,024 reflections between 6.0 and 1.93 Å resolution. The atomic coordinates will be deposited in the Brookhaven Protein Data Bank.

Acknowledgments

This work was supported by an Ohio Regent's Eminent Scholar award to M.S. and an NIH grant (GM41788) to M.-D.T. We gratefully thank the Ohio State Supercomputer Center for the computer time on the Cray Y-MP/864. This paper is No. 8 (for No. 7 see Dupureur et al. [1992b]) in the series "Phospholipase A_2 engineering" and No. 2 (for No. 1 see Noel et al. [1991]) in the series on "Crystallography of phospholipase A_2."

References

Brunger, A.T. (1990). *XPLOR Manual.* Yale University, New Haven, Connecticut.

Brunie, S., Brolin, J., Gerwirth, D., & Sigler, P.B. (1985). The refined crystal structure of dimeric phospholipase A_2 at 2.5 Å. Access to shielded catalytic site. *J. Biol. Chem. 260*, 9742–9749.

Dijkstra, B.W., Drenth, J., & Kalk, K.H. (1981a). Active site and catalytic mechanism of phospholipase A_2. *Nature 289*, 604–606.

Dijkstra, B.W., Kalk, K.H., Drenth, J., de Haas, G.H., Egmond, M.R., & Slotbum, A.J. (1984). Role of the N-terminus in the interaction of pancreatic phospholipase A_2 with aggregated substrates. Properties and crystal structure of transaminated phospholipase A_2. *Biochemistry 23*, 2759–2766.

Dijkstra, B.W., Kalk, K.H., Hol, W.G.J., & Drenth, J. (1981b). Structure of bovine pancreatic phospholipase A_2 at 1.7 Å resolution. *J. Mol. Biol. 147*, 97–123.

Dupureur, C.M., Li, Y., & Tsai, M.-D. (1992a). Phospholipase A_2 engineering. 6. Single amino acid substitutions of active site residues convert the rigid enzyme to highly flexible conformational states. *J. Am. Chem. Soc. 114*, 2748–2749.

Dupureur, C.M., Yu, B.-Z., Jain, M.K., Noel, J.P., Deng, T., Li, Y., Byeon, I.-J., & Tsai, M.-D. (1992b). Phospholipase A_2 engineering. Structural and functional roles of highly conserved active site residues tyrosine-52 and tyrosine-73. *Biochemistry 31*, 6402–6413.

Heinrikson, R.L., Krueger, E.T., & Keim, P.S. (1977). Amino acid sequence of phospholipase A_2-α from the venom of *Crotalus adamanteus*. A new classification of phospholipase A_2 based on structural determinants. *J. Biol. Chem. 252*, 4913–4921.

Howard, A.J. (1988). *A Guide to Macromolecular X-ray Data Reduction for the Nicolet Area Detector Systems. Version 1.3.* Protein Engineering Department, Genex Corporation, Maryland.

Maraganore, J.M., Poorman, R.A., & Heinrikson, R.L. (1987). Phospholipase A_2: Variations on the structural theme and their implications as to mechanism. *J. Protein Chem. 6*, 173–189.

Noel, J.P., Bingman, C.A., Deng, T., Dupureur, C.M., Hamilton, K.J., Jiang, R.-T., Kwak, J.-G., Sekharudu, C., Sundaralingam, M., & Tsai., M.-D. (1991). Phospholipase A_2 engineering: X-ray structura and functional evidence for the interaction of Lys-56 with substrates *Biochemistry 30*, 11801–11811.

Scott, D.L., White, S.P., Otwinowski, Z., Yuan, W., Gelb, M.H., & Sigler, P.B. (1990). Interfacial catalysis: The mechanism of phospholipase A_2. *Science 250*, 1541–1546.

van den Bergh, C.J., Bekkers, A.C.A.P.A., de Geus, P., Verheij, H.M. & de Haas, G.H. (1987). Secretion of biologically active porcine phospholipase A_2 by *Saccharomyces cerevisiae. Eur. J. Biochem 170*, 241–246.

Verheij, H.M., Slotboom, A.J., & de Haas, G.H. (1981). Structure and function of phospholipase A_2. *Rev. Physiol. Biochem. Pharmacol 91*, 91–227.

White, S.P., Scott, D.L., Otwinowski, Z., Gelb, M.H., & Sigler, P (1990). Crystal structure of cobra-venom phospholipase A_2 in complex with a transition state analogue. *Science 250*, 1560–1563